Taylor & Francis
Taylor & Francis Group

Fullerenes, Nanotubes and Carbon Nanostructures

ISSN: 1536-383X (Print) 1536-4046 (Online) Journal homepage: https://www.tandfonline.com/loi/lfnn20

Aqueous fullerene C_{60} solution suppresses herpes simplex virus and cytomegalovirus infections

Regina Klimova, Sergey Andreev, Ekaterina Momotyuk, Natalia Demidova, Natalia Fedorova, Yana Chernoryzh, Kirill Yurlov, Evgeny Turetskiy, Elena Baraboshkina, Nadezhda Shershakova, Ruslan Simonov, Alla Kushch, Musa Khaitov & Alexander Gintsburg

To cite this article: Regina Klimova, Sergey Andreev, Ekaterina Momotyuk, Natalia Demidova, Natalia Fedorova, Yana Chernoryzh, Kirill Yurlov, Evgeny Turetskiy, Elena Baraboshkina, Nadezhda Shershakova, Ruslan Simonov, Alla Kushch, Musa Khaitov & Alexander Gintsburg (2019): Aqueous fullerene C_{60} solution suppresses herpes simplex virus and cytomegalovirus infections, Fullerenes, Nanotubes and Carbon Nanostructures, DOI: 10.1080/1536383X.2019.1706495

To link to this article: https://doi.org/10.1080/1536383X.2019.1706495

Published online: 30 Dec 2019.

FULLERENES, NANOTUBES AND CARBON NANOSTRUCTURES
https://doi.org/10.1080/1536383X.2019.1706495

Aqueous fullerene C_{60} solution suppresses herpes simplex virus and cytomegalovirus infections

Regina Klimova[a], Sergey Andreev[b], Ekaterina Momotyuk[a], Natalia Demidova[a], Natalia Fedorova[a], Yana Chernoryzh[a], Kirill Yurlov[a], Evgeny Turetskiy[b,c], Elena Baraboshkina[b], Nadezhda Shershakova[b], Ruslan Simonov[a], Alla Kushch[a], Musa Khaitov[b], and Alexander Gintsburg[a,c]

[a]Gamaleya NRC for Epidemiology and Microbiology, Ministry of Health of the Russian Federation, Moscow, Russian Federation; [b]NRC Institute of Immunology FMBA of Russia, Moscow, Russian Federation; [c]Sechenov First Moscow State Medical University, Moscow, Russian Federation

ABSTRACT

Fullerene C_{60} is known as a promising therapeutic agent due to its antioxidant, anti-inflammatory and other properties, along with the lack of noticeable toxicity. In this article, we describe antiviral properties of aqueous fullerene C_{60} dispersion (ndC_{60}) produced by biocompatible diafiltration technology and C_{60} amino derivatives against Herpes simplex virus type 1 (HSV-1) and Human cytomegalovirus (HCMV) infections. Their activity *in vitro* was evaluated by a plaque reduction assay using Vero and HF cells in pre- and post-treatment modes. Therapeutic efficacy of dnC_{60} and C_{60} derivatives was studied in DBA mice using cutaneous model of HSV-1 infection. Data obtained indicated low cytotoxicity of all used compounds for both cell lines ($CC_{50} > 1$ mg/ml). The antiviral activity of dnC_{60} in most tests exceeded the activity of both C_{60} amino adducts and acyclovir (ACV), and it demonstrated significant therapeutic effect against HSV-1 skin infection in mice.

ARTICLE HISTORY
Received 11 December 2019
Accepted 16 December 2019

KEYWORDS
Aqueous C_{60} dispersion; C_{60} adducts; Herpes simplex virus; Human cytomegalovirus; antiviral activity

1. Introduction

Herpes simplex viruses type 1 (HSV-1) and type 2 (HSV-2) and human cytomegalovirus (HCMV) are common pathogens in the human population. According to estimates of the World Health Organization (WHO) in the world about 3,7 billion people with age to 50 years (67% of the population in this age bracket) are infected with HSV-1 while 417 million people with age from 15 to 49 years (11% of the population) – by HSV-2.[1] The prevalence of HCMV infection varies significantly in different regions of the world from 45% to 100%.[2] Among the population of Russia about 20 million of new cases of herpesvirus infections are registered annually. Primary infection and reactivation of human herpesviruses (HHV) from latent state causes serious illness including cases with lethal outcome. These infections are especially hazardous for persons with decreased immunity: newborns, pregnant women, HIV-infected patients and patients after organ and tissue transplantations.

The main methods of treatment of herpesviruses diseases are aimed to repress the viral reproduction in the body but they are unable to suppress the virus being present in a latent form. Well-known specific antiviral drugs acyclovir (ACV), ganciclovir (GCV) and their analogs that are applied for treatment of HHV infections have a number of drawbacks. The most significant ones include toxicity and resistance of viruses which increases with prolonged use and with recurrent diseases.[3–5] In this regard, the urgent task is the development of new drugs against HHV with different mechanisms of action that would also be effective against wild-type viruses and mutant drug-resistant strains of HSV-1/2 and HCMV. In addition, an important issue is the design of drugs that can prevent the penetration of the virus into the body through the skin and mucous membranes.

Currently, a large interest of researchers has been focused on fullerene C_{60} and its water-soluble derivatives. Fullerene C_{60} in water-soluble forms (C_{60} nanodispersion, dnC_{60}) possesses low toxicity and withal permeability through biological membranes.[6] The dnC_{60} and some C_{60} derivatives (adducts) exhibit *in vitro* antioxidant and antiviral properties[7–13] including activity against herpetic infection.[10] The development of fullerene-based drugs for the treatment of various diseases, including HSV-1/2 etiology, is being actively developed.[10,11,13] However, the widespread use in medicine of these compounds is significantly hampered by the high cost of their synthesis and problems in their purification; another problem is the uncertainty in their toxicological properties. Therefore, a design of low-cost fullerene-based drug against viral infections with low toxicity and possibility to scale its production is a desirable task. In principle, an aqueous dispersion of unmodified fullerene is suitable substance for this role, since there are many publications on the chemical and biological properties of this form[14–22] indicating its low toxicity. Recently, some of the

CONTACT Sergey Andreev sm.andreev@nrcii.ru NRC Institute of immunology FMBA of Russia, Kashirskoye shosse, 24, Moscow, 115478 Russian Federation.
Color versions of one or more of the figures in the article can be found online at www.tandfonline.com/lfnn.

authors of this publication have described[15] a new method for preparing an aqueous C_{60} dispersion using a biocompatible diafiltration method, in contrast to the traditional toluene/ultrasonic method.[23,24] Studies have been shown that dnC_{60} is promise anti-inflammatory agent (atopic dermatitis and other allergic diseases) in the absence of toxicity.[22,25] On the other hand, it is known that C_{60} have potential antiviral activity against enveloped viruses and what is more the mechanisms for virus inactivation may vary.[11,26,27]

The purpose of this work was to study the antiviral activity of dnC_{60} against HSV-1 and HCMV infections in cell cultures, as well as *in vivo* upon cutaneous HSV-1 infection in mice.

2. Materials and methods

2.1. dnC_{60} preparation

The dnC_{60} was produced by a diafiltration method as described[15] in a modified version using tangential ultrafiltration instead of dialysis. Briefly, 80 mg of pristine fullerene C_{60} powder (NeoTec product, Russia 99.95%) was dissolved in 100 ml of N-methyl-1-pyrrolidone (NMP, Sigma Aldrich, 99.5%) and obtained purple solution was then passed through glass fiber filter (Sigma Aldrich, 2.6 µm) and 100 ml of distilled water was added to the filtrate. An exchange solution was deionized water (other variant is pluronic F-128, 0.01% in water). Obtained solution was subjected to tangential flow filtration (TFF) using peristaltic pump (Spectrumlabs Krosflo ACR1-U20-01N) with performance 15–200 ml/min and ultrafiltration modules Sartorius Vivaflow 50 with 100 kDa membrane ("regenerated cellulose"). The process of removing NMP from C_{60}-containing retentate was monitored by spectrophotometry by the quantification of NMP in permeate, and was finalized after the practical disappearance of band at 190–210 nm which characteristic for free NMP absorption. The final solution was filtered through 0.45 µm pores resulting in a clear transparent brownish solution dnC_{60} stored at 4 °C protected from light exposure. Elemental analysis of vacuum-dried sample (%): C 78.62, H 1.11, N 2.28. The fullerene content was quantified by spectrophotometry (Cary 100, Agilent Technologies, 10 mm cell) using a calibration curve and measured value of its molar extinction coefficient at 340 nm ($\mathcal{E} = 50200$). The concentration of fullerene in dnC_{60} used in this work was approx. 1 mg/ml.

2.2. C_{60}-amine adducts

The water-soluble C_{60} adducts with L-arginine (C_{60}-Arg), L-lysine (C_{60}-Lys) and piperazine (C_{60}-Pip) were synthesized as described below.

2.2.1. C_{60}-Lys

To a solution of 862 mg (3.5 mmol) of N-ε-Boc-L-Lysine (Merck) in 10 ml of DMSO was added 2.57 ml of 20% tetraethylammonium hydroxide solution (Merck) and 30 min after 50 mg (0.069 mmol) of fullerene C_{60}. The resulting dispersion was stirred for 24 hours until homogeneous, TLC (Kiesel gel 60/DMF: toluene (1: 1)) indicated the absence of free fullerene. The color of the solution was greenish brown. The solution was diluted with 50 ml dist. water and acidified to pH 3, and after 15 min, the loose loose precipitate was filtered (0.45 µm) and dried in vacuum. Dry powder (188 mg) was treated with a 50% (v/v) solution of trifluoroacetic acid (TFA) in methylene chloride for 15 min. Then the mixture was evaporated in vacuo, the residue was washed four times from TFA traces with dry diethyl ether (by decantation), and the residue obtained was dried in vacuo. The resulting brown powder (67 mg) shows good solubility in water, the pH of the solution is close to neutral. Elemental analysis (%): C 44.60, H 3.31, N 5.64; calculated nitrogen-based molar ratio for C_{60}/Lys was ~1/4-5. The acid-base titration indicated the presence of approximately 5 basic groups/C_{60}. FTIR spectra, major bands: 3300–3500 (broad), 2400–2300, 1680 (s), 1428, 1202 (s), 1138 (s) cm^{-1}.

2.2.2. C_{60}-Arg

8.8 ml (36 mmol) of N, O-Bis-(trimethylsilyl)-acetamide (Merck) were added to a suspension of 1.74 g (10 mmol) of L-arginine in 20 ml of NMP, and the mixture was stirred until a yellowish solution was obtained (approximately 12 hrs). Then, 144 mg (0.2 mmol) of fullerene C_{60} was introduced into the reaction mixture and stirred for 18 hours at room temperature. In the next step, 50 ml of distilled water was added to the mixture, followed by dialysis against water. The aqueous phase was acidified to pH 3 (1 N HCl) and then the solution was evaporated under vacuum on a rotary evaporator at 40°C to remove the hexamethyldisilane formed. The remaining aqueous solution was passed through a 0.22 µm filter and further, the isolation procedure was analogous to that described above. The yield of water-soluble brown powder was 370 mg. Elemental analysis of vacuum-dried sample (%): C 51.69, H 3.71, N 12.96; calculated molar ratio for C_{60}/Arg was 1/4-5. FTIR spectra: 2400–2300, 1675, 1400, 1075 cm^{-1}.

2.2.3. C_{60}-Pip

50 mg of fullerene C_{60} were dissolved in 50 ml of toluene (99.9%, Panreac Applichem) and then 1 ml of DMSO and 129 mg of Boc-piperazine (98%, Sigma) were added. Resulting mixture was agitated on magnetic stirrer for 1.5 hours, until initial purple solution had turned brown. The reaction mixture was then evaporated in high vacuum to remove above solvents and treated by 1:1 mixture of dichloromethane (DCM, 99.8%, Sigma) and trifluoroacetic acid (TFA, 99%, Sigma) for 15 min. Thr mixture has been concentrated in vacuo to remove DCM and TFA. Obtained residue was washed several times with dry ethyl ether (99%, Sigma) to remove traces of TFA and vacuum dried. The yield of light brown powder (C_{60}-Pip) was 162 mg, its aqueous solution had an intense orange color. Elemental analysis of vacuum-dried sample (%): C 71.55, H 5.22, N 10.43; calculated molar ratio for C_{60}/Pip was ~1/4-5. FTIR spectra: 2400–2300, 2477 (s), 1666 (s), 1482, 1433, 1075, 725 cm^{-1}.

2.3. Spectral and elemental analysis

UV-VIS absorption spectra were recorded on a double beam spectrophotometer Cary 100 (Agilent Technologies) in the range of 190–800 nm using 1-cm quartz cell. FTIR spectra were recorded on a Bruker Alpha IR spectrometer (attenuated total reflectance (ATR) measurements) using freeze-dried samples of nC_{60}. Measurements of C_{60} nanoparticle sizes and ξ-potential were performed by dynamic light scattering (DLS) using a Photocor Compact-Z instrument (Photocor, Russia). Elemental analysis has been performed by 2400 series II Perkin Elmer element analyzer.

2.4. Electron microscopy measurements

Samples of dnC_{60} were taken on a scanning electron microscope (SEM) TESCAN MIRA 3 LMH equipped with field emission cathode (Schottky emitter). Scan options: primary electron beam energy is 5 keV with beam current 130 pA. For registration of the signal, a secondary electron detector was used. Samples were dried in vacuum prepared without any sputtering with conductive layer.

2.5. Cell cultures

Vero cells (African green monkey kidney) and HF cells (human fibroblasts) were used in the present work. Vero cells were grown in Eagle's minimum essential medium (MEM), HF cells – in Dulbecco's modified Eagle medium (DMEM) supplemented with 2 mM L-glutamine, 50 µg/mL gentamicin and 10% fetal bovine serum (FBS). All reagents were purchased from Paneco (Moscow, Russia).

2.6. Viruses

HSV-1 (F) and HCMV (AD169) were obtained from the State Virus Collection of the Gamaleya NRCEM (Moscow, Russia). Viruses were propagated and titrated on Vero cells (HSV-1) and HFs (HCMV). Virus titers were quantified by plaque assay.

2.7. Cytotoxicity assay

Cytotoxicity of compounds was tested by standard MTT method. Briefly, Vero and HF cells cultivated in 96 well microplates with compound in serial dilutions for 72 hours at 37 °C in 5% CO_2 atmosphere. Further the medium was replaced with 50 µl of a 1 mg/ml solution of MTT [3-(4,5-dimethylthiazol-2-yl)-2,5-diphenyl tetrazolium bromide) in Eagle-MEM. Cells were incubated at 37°C for 3 hours, and 100 µl of acid-isopropanol (0.1 N HCl in isopropanol) was added to each well. After a few minutes at room temperature to ensure that all crystals were dissolved, the plates were read using an automatic plate reader (TECAN, Switzerland) with a 570 nm test wavelength and a 690 nm reference wavelength. The 50% cytotoxic concentration (CC_{50}) was defined as the compound concentration that caused a 50% reduction in the number of viable cells.

2.8. Positive treatment control

Acyclovir (ACV, Zovirax®, Glaxo Wellcome Operations, Great Britain) was used as a positive control in the *in vitro* experiments with HSV-1-infection, while in the *in vivo* experiments 5% Acyclovir ointment (ACV-A, OOO Akrikhin, Moscow region, Russia) for external use, and Ganciclovir (GCV, Cimeven®, Hoffman-La Roche, Switzerland) were used.

2.9. Antiviral activity assay

The antiviral activity of test compounds was evaluated by a standard plaque reduction assay. The different concentrations of compounds were added to Vero and HF cells prior (pretreatment assay) or post (post-treatment assay) viral infection.

2.9.1. Pretreatment assay

Monolayer of Vero and HF cells were covered by the cultural medium containing the different concentrations of compounds and incubated for 24 hours at 37 °C under 5% CO_2. After 24 hours, Vero cells were infected with HSV-1 at 0.01 plaque forming units per cell (PFU/cell) and HF cells were infected with HCMV at 0.001 PFU/cell for 1 hour at 37°C under 5% CO_2. Further, the cells were twice washed with phosphate buffered saline (PBS) and placed into the maintenance medium (MEM with 2% FBS) and incubated under the conditions described above.

2.9.2. Post-treatment assay

Cell monolayers were infected with HSV-1 or HCMV and incubated for 1 hour under the conditions described above. Then the cells were twice washed with PBS and the different concentrations of compounds were added.

2.9.3. Virucidal activity assay

The viruses were mixed with the test compounds at different concentrations and incubated for 1 hour at 37 °C. Then the incubation mixture (virus plus compounds) was applied to the cell monolayers and incubated for 1 hour at 37 °C under the conditions described above. The cell monolayers were washed and the culture medium with 2% FBS was added.

The data were analyzed and presented as the means of triplicates ± SD for each dilution. ACV or GCV at concentrations of 44 µM and 19.6 µM, respectively, were used as positive controls, not treated infected cells were used as virus controls. The plaque inhibition rate was calculated by Spearman-Karber method as previously described.[28] The IC_{50} (50% inhibitory concentration) for test compounds was calculated by regression analysis. The selectivity index (SI) of compounds was calculated as the ratio of CC_{50} to IC_{50}.

2.10. Analysis of CMV mRNA expression

Seven days after infection with HCMV, HF cells treated with dnC_{60} at a concentration of 500 μg/ml were lysed by TRIzol Reagent (Thermo Fisher Scientific, USA) and total RNA was isolated according to the protocol of the manufacturer (Thermo Fisher Scientific, USA). Infected cells not treated with dnC_{60} and uninfected cells were used as positive and negative controls, respectively. After isolation of RNA, samples were treated with DNase (Thermo Fisher Scientific, EN0525). Synthesis of cDNA was performed using RevertAid H Minus Reverse Transcriptase (Thermo Fisher Scientific, EP0452) according to the manufacturer's appropriate protocols. To identify the mRNA of corresponding the HCMV genes UL122, UL83, UL54 and the GUS gene as reference housekeeping gene the primers used were:

UL122-F	TCATGTTGCGGTAATCGGAGGAACG
UL122-R	CACAGCCGATGCTTGTAACGAAGG
UL83-F	TGCCCTGGATGCGATACTG
UL83-R	AGGACCTGACGATGACCCG
UL54-F	GCGTACCGTTGAAAGAAAAGCATAAAGC
UL54-R	GCACTTCGGAGGGTGTGATCTTTGG
GUS-F	CGTGGTTGGAGAGCTCATTTGGAA
GUS-R	ATTCCCCAGCACTCTCGTCGGT

For PCR assay LightCycler® 480 Real-Time PCR System (Switzerland, Roche) was used. The results of RT-PCR were determined relative to the GUS gene.

2.11. Therapeutic efficacy

Female DBA/2J (H-2d) mice ages 6–10 weeks were purchased from the animal nursery Filial SCBMT "Stolbovaya" (Moscow region, Russia) and kept in a pathogen-free environment with an OVA-free diet. All experimental procedures were carried out according to order no.708 of the Ministry of Health of the Russian Federation and "Regulations on the ethical attitudes to laboratory animals of N.F. Gamaleya NRCEM (Moscow, Russia)."

The back areas of the mice (1 × 1 cm) were chemically depilated. One day later, the naked skin was scratched and 0.1 ml of HSV-1 suspension of 1×10^6 PFU/ml was applied in scarified area. After 24 hours of virus challenge mice of group 1 (n = 5) were treated with 0.1 ml of dnC_{60} (10 μg/mouse), group 2 (n = 5) using 0.1 ml of C_{60}-Pip (50 μg/ml), group 3 (n = 8) using ACV ointment (5000 μg ACV/mouse). Mice of the control group 4 (n = 8) received 0.1 ml of saline each. All test compounds were applied to the skin one time daily for 3 days. The observations were conducted daily, the results of the treatment were analyzed by evaluating the development of HSV-1- specific skin lesions for 10 days and were scored from 0 to 6 as described.[29,30]

2.12. Determination of antiviral antibodies

Anti-HSV-1 antibody titers in mouse sera were measured by ELISA as described earlier.[31] Briefly, the 50 μg/ml HSV-1 antigen ("Vecto-HSV-1,2-IgG," Vector, Koltsovo, Russia) was adsorbed into a 96-well plate by incubation for 18 hours at 37 °C. The plates were washed and sera were added at various dilutions (sera of mice in each group were pooled). After washing, anti-mouse IgG antibodies labeled with peroxidase (Dako, Denmark) were added to the wells. The optical density was evaluated using a microtiter plate reader Multiskan (TECAN, Switzerland) at a wavelength of 450 nm.

2.13. Statistical analysis

The statistical analysis was performed using the GraphPad Prizm 5.0 software package. Student's *t*-test (*t*-test) was used to calculate and compare mean values, and analysis of variance of ANOVA was used to analyze differences in the clinical manifestations of HSV-1 infection between groups. Differences were considered statistically significant at $p < 0.05$.

3. Results

3.1. dnC_{60}

The method described here for obtaining a fullerene water dispersion dnC_{60} is quite different from the well-known traditional method involving the long-term ultrasonic treatment of a heterogeneous mixture of water/C_{60} solution in toluene.[24] This diafiltration protocol does not use toxic solvents (toluene) and heating, and it allows to adjust the concentration of C_{60} to record values (up to 1 g/L). However, the method allows to obtain solutions with concentrations of fullerene C_{60} up to 2 g/l if a 0.01% solution of pluronic F-127 is used as a displacing medium instead of pure water. Study of its physicochemical properties demonstrated that the dispersion contains C_{60} clusters with hydrodynamic radius ~80–100 nm and with net negative surface charge (z-potential) – 25–30 mV (Figure 1). SEM images of dried dnC_{60} samples demonstrated approximately 100 nm agglomerates consisting of small particles with the size of about 15–30 nm (Figure 2). The small angle X-ray neutron scattering data indicated a two-level aggregation of particles in the dnC_{60} dispersion, fullerene molecules initially collected in dense aggregates several nanometers in size, and then they are associated in secondary fractal aggregates.[32] According to elemental analysis (Table 1) the vacuum dried dnC_{60} samples (at 10 μm of Hg, 24 hrs) contained a nitrogen due to the presence of NMP forming with fullerene a charge transfer complex (CTC).[13] We suppose that the C_{60} clusters are apparently surrounded with tightly bound water shell not removable in high vacuum. FTIR spectrum (Figure 3) of dried dnC_{60} displays four bands characteristic for fullerene skeleton at 1427, 1181, 575 and 525 cm^{-1}, in addition it contains other bands associated with the presence of bound water (3500–3200), NMP complexed to C_{60} (2917 and 1598, C–H and C = O), and of possibly OH groups (C–O bond, 1000–1180 cm^{-1}). The possibility of minor hydroxylation of fullerene in aqueous dispersions was described also by other authors.[14,15,18] UV-Vis absorption spectrum of dnC_{60} is characterized by three intensive maxima at 222, 268 and 340–347 nm and less intensive broad band at about 400–600 nm (Figure 4). The comparative

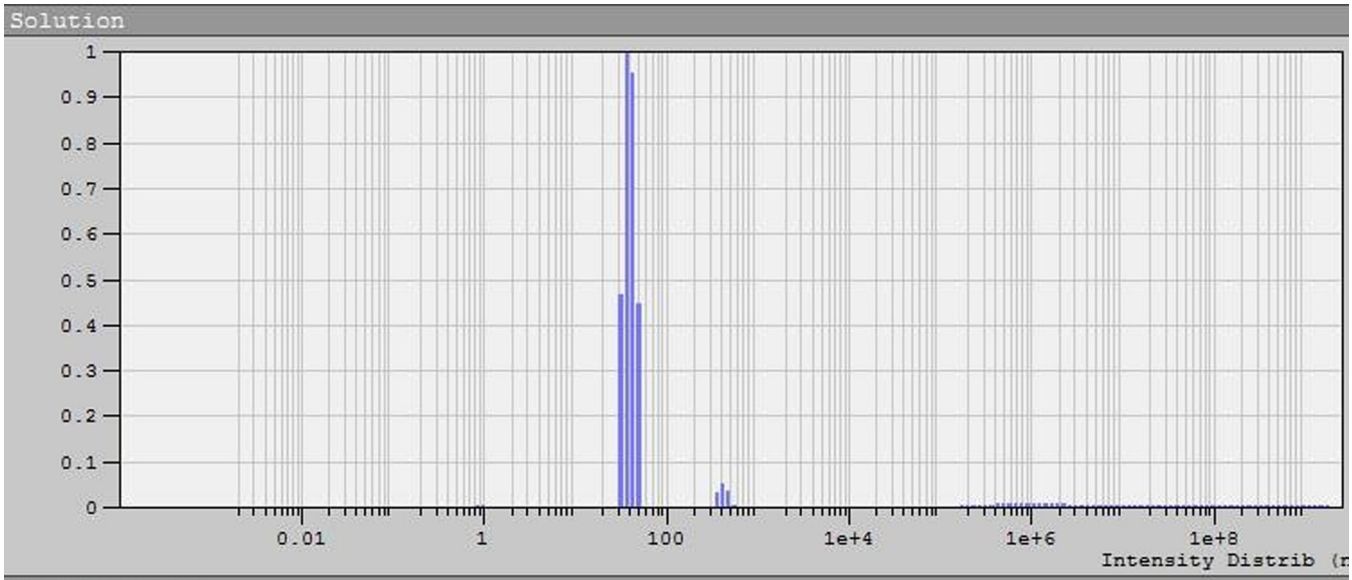

Figure 1. Size distribution (radius) of fullerene C_{60} particles in aqueous dispersion dnC_{60} recorded on Photocor Compact Z nanoparticle analyzer.

thin-layer chromatographic analysis of ndC_{60} and C_{60} in toluene on a silica gel plates (eluent dimethylformamide: toluene (1:1)) demonstrated different behavior of C_{60}. In the first case, the main spot was observed near the start, while in the second case near the front. The mass spectra of the extracted substance from the spots showed only molecular ion C_{60}. These results demonstrate the absence of a noticeable chemical modification of fullerene in dnC_{60}. Final concentration of the C_{60} in the dnC_{60} was approx. 1 g/L (~1.39 mM). A good thermostability of dnC_{60} allows using of sterilization.

3.2. C_{60} adducts

The amino acid trimethylsilyl (TMS) derivatives were used in the synthesis of C_{60} amino acid adducts, which allowed the reaction to be carried out in a homogeneous aprotic medium, where then the removal of TMS groups is easily achieved by water.[33] The C_{60}/piperazine adduct was prepared using mono-protected (Boc)-piperazine. This substance was good soluble in water at pH <7.5 (>50 mg/ml, orange color); its solution in dist. water shows an pH ~ 3 (salt of a weak base and a strong acid). Earlier, C_{60} tetrapiperazine derivative was obtained in another way by Japanese researchers described as a highly water-soluble substance with an orange color in solution.[34] Other C_{60} adducts, with Arg and Lys, were sparingly soluble at neutral pH and good at low pH (>3 mg/ml); Belstein's chlorine test gave a positive reaction. The adducts were characterized by elemental analysis, particle size and surface charge, UV and FTIR spectra. In dry form after freeze drying they are as brown powders. Obviously also, they all also contained a certain amount of water as indicated by elemental analysis and FTIR spectra. It should be noted that the C_{C60}–H fragment formed after the formation of the adduct can undergo oxidation in air and then turn into hydroxyl. Mass spectra/MALDI-TOF showed the presence of mono-, bis-, tris-addition of amino addends together with C_{60} ion (m/z ~ 720) (Figure 5). However, it is known that fullerene adducts with $C_{(C60)}$–N covalent bonds are thermally unstable,[35] and even with a mild ionization method only a peak with m/z 720 is often present in the mass spectrum. It is rarely

possible to establish the number of attached addends by mass spectrometry due to the decay of molecules under the influence of a laser strike. Unfortunately, good NMR spectra could not be obtained because of self- association of C_{60} derivatives in aqueous medium. The UV spectra of these derivatives does not have noticeable maxima, they look like a smoothed curve (not shown), and this is typical for spectra of many C_{60}-amine addition products.[15] The DLS measurements of C_{60}-Arg, C_{60}-Lys and C_{60}-Pip showed that their main dimensions lies in the region about 10–55, 18–60, 55–150 nm, respectively, however there are also observed and more large aggregates. For instance, solutions

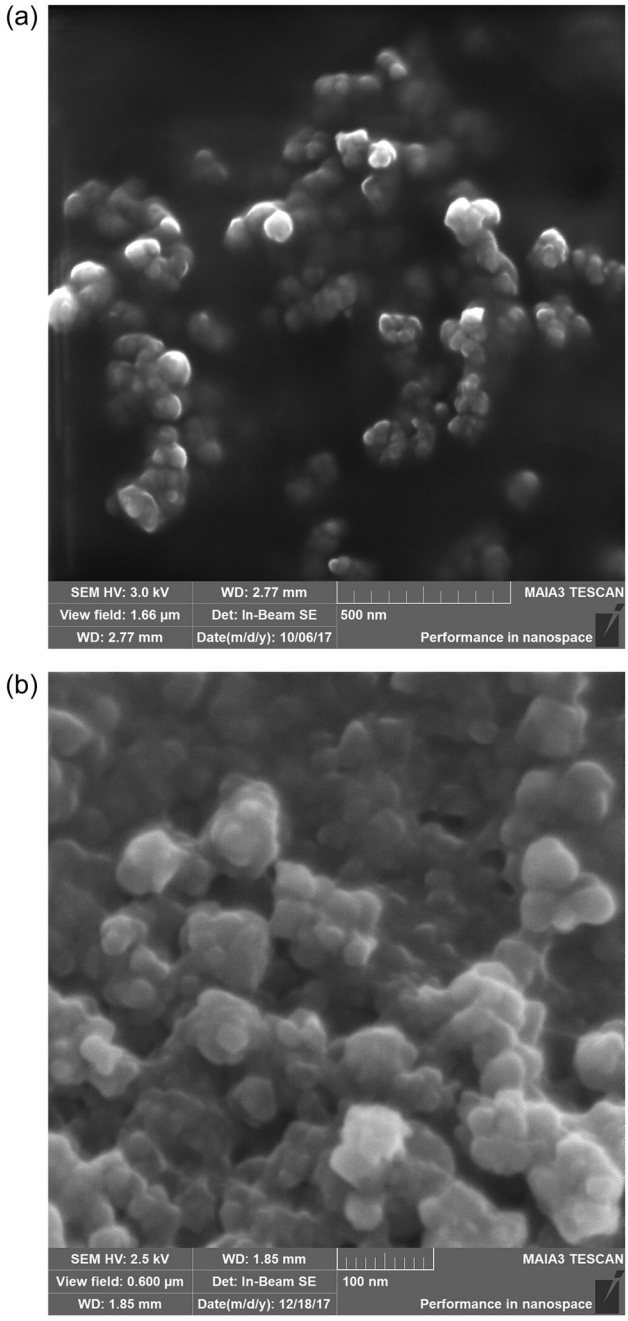

Figure 2. SEM images of dnC_{60} dried in vacuum: (a) view field 1.66 µm; (b) view field 0.6 µm.

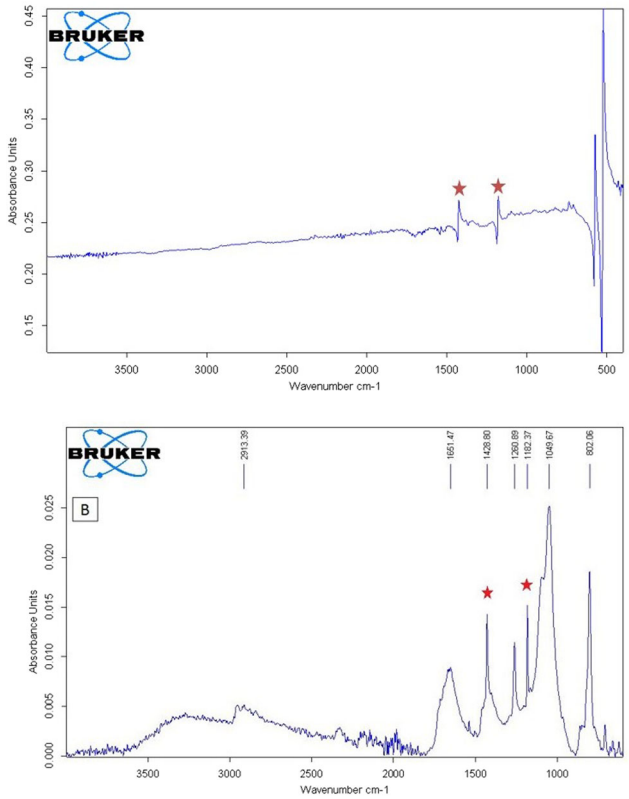

Figure 3. FTIR spectra of pristine C_{60} (upper) and ndC_{60} vacuum dried.

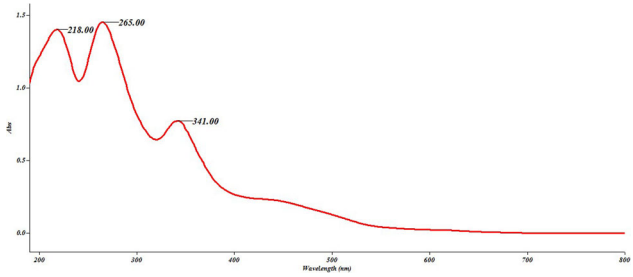

Figure 4. UV-Vis absorption spectrum of dnC_{60}.

Table 1. Cytotoxicity and anti-HSV-1 effect for tested compounds.

		Assays					
		Pre-treatment		Post-treatment		Virucidal	
Compounds	CC_{50}*	IC_{50}**	SI***	IC_{50}	SI	IC_{50}	SI
dnC_{60}	172 ± 0.7	0.8 ± 0.02	**215 ± 5.5**	1.3 ± 0,02	**132 ± 0.3**	0.1 ± 0.02	**1720 ± 312**
C_{60}-Arg	55.9 ± 0.3	0.6 ± 0.01	93 ± 1.3	–#	–	–	–
C_{60}-Lys	57.7 ± 0.4	0.5 ± 0.01	**107 ± 1.2**	–	–	4.6 ± 0.01	12.5 ± 0.2
C_{60}-Pip	61.9 ± 0.6	0.4 ± 0.01	**155 ± 4**	1.8 ± 0.06	34 ± 1.8	–	–
ACV	4444 ± 32	3.2 ± 0.1	**1388 ± 48**	0.6 ± 0.3	**7406 ± 78**	11.1 ± 0.1	**400 ± 13.6**

*50% cytotoxic concentration, the means ± SD, µM/ml; **50% inhibiting concentration, the means ± SD, µM/ml; ***selective index CC_{50}/IC_{50}; #no detected; bold – SI > 100.

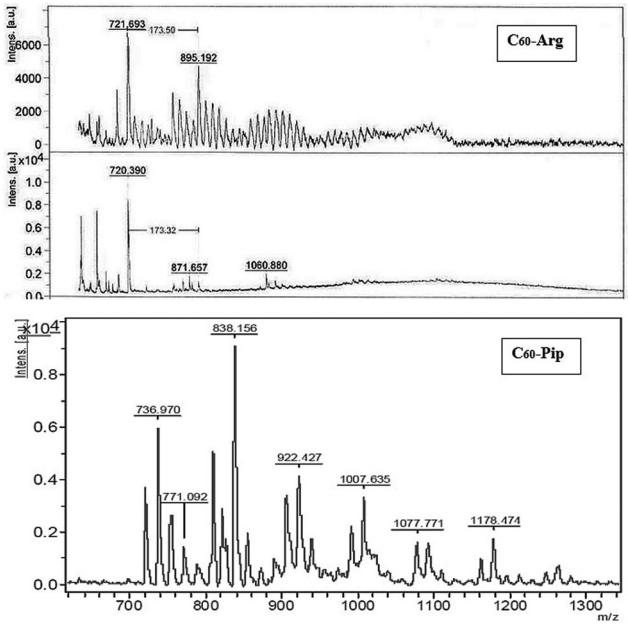

Figure 5. Mass spectrum (MALDI-TOF) of C_{60}-Arg and C_{60}-Pip.

of C_{60}-Arg, in contrast to dnC_{60}, contain fractions of non-associated primary aggregates with size of few nanometers.[32] The surface charge of the adducts had a positive sign indicating the presence of cationic species with ζ-potentials: 22.0 ± 4.31 (C_{60}-Arg), 16 ± 4.00 (C_{60}-Lys) and 60.6 ± 8.23 (C_{60}-Pip). The high charge for the latter compound explains its very high solubility. The molar ratio addend: C_{60} was calculated on the basis of elemental analysis of dried in high vacuum samples taking into account the nitrogen content, the data were as follows: C_{60}-Arg ~4–5, C_{60}-Lys ~4–5 and C_{60}-Pip ~4–5. The nominal molecular weights of C_{60} substances were calculated based on the C_{60} content. All FTIR spectra of the adducts demonstrated the presence of strong band near 3300–3500 cm^{-1} probably indicating the presence of an attached OH group and/or water molecules.

3.2.1. Cytotoxicity test

To assess the cytotoxicity of C_{60} substances, Vero cells were incubated with each substance at different concentrations (ranges 50–500 μM). The value of CC_{50} for dnC_{60} was 172 ± 0.7 μM, while all C_{60} amino adducts had almost the same value, demonstrating toxicity more than doubled compared to dnC_{60} (Table 1). Thus, dnC_{60} showed markedly lower toxicity for Vero cells compared to the C_{60} derivatives used ($p < 0.001$). Note, we could not determine the CC_{50} of dnC_{60} for HF cells even at the maximum concentration used (138.8 μM).

3.2.2. Antiviral activity in vitro

The results of the analysis of the *in vitro* antiviral activity of C_{60} compounds are presented in Figure 6. In pretreatment mode assay, all compounds significantly suppressed HSV-1 infection, maximal effect was shown for dnC_{60} (87 ± 2.6%) meanwhile for ACV it was noticeably less (37 ± 2.6%) ($p < 0.001$, Figure 6(a)). In post-treatment mode, only ACV and dnC_{60} were able to inhibit the HSV-1 infection, by 93 ± 5.6% and 60 ± 4.4%, respectively (Figure 6(b)). In virucidal assay, only dnC_{60} displayed the high activity inhibiting infection in Vero cells by 98.2 ± 1.8% ($p < 0.001$) (Figure 6(c)), while other compounds, including ACV, demonstrated no or weak activities against HSV-1. To calculate the IC_{50} values the graphs of dependence of inhibition of HSV-1 infection on various concentrations of the tested compounds are plotted. In Figure 7(a–c), the graphs for calculating the IC_{50} for dnC_{60} are shown. The IC_{50} for the remaining compounds were determined in a similar way. The calculated IC_{50} and SI (selectivity index) are given in Table 1.

With regard to the effects of these compounds on the HCMV, at concentrations 7 and 1.4 μM, the dnC_{60} inhibited the virus both prior to (82 ± 4.6% and 57 ± 1%, respectively) and after (80 ± 2.6% and 27 ± 1%) infection of cells (Figure 6(d)). However, at these concentrations dnC_{60} displayed no HCMV-virucidal activity (open column, Figure 6(d)). IC_{50} (M ± SD) determined by linear regression was 0.01 ± 0.008 μM for prior-infection and 0.04 ± 0.0037 μM for post-infection assay (Figure 7(a,b)). Anti-HCMV activity of dnC_{60} was dose-dependent both in pre- and post-treatment assays (Figure 7(c)).

3.2.3. Therapeutic efficacy

Two selected compounds were tested in a mouse model of cutaneous HSV-1 infection. Substances dnC_{60} and C_{60}-Pip were applied topically to the sites of the infection; ointment containing 5% ACV was used as a positive control. The results were analyzed according to the decrease of HSV-1-specific skin lesion and presented as scores. The scores corresponding to specific clinical manifestations are illustrated by photos in Figure 8. In control mice (group 4), clinical manifestations of HSV-1 infection reached the maximum on days 3 and 6: with scores 3.85 ± 0.27 and 3.75 ± 0.2, respectively (Figure 9(a)). On days 5–7 two out of eight mice died (25%), on day 10 only infrequent erosions (scores 2 ± 0.1) were observed in survived mice. In groups 1–3, none of mice died throughout the entire period of observation. Skin damage was minimal in animals treated with dnC_{60} and ACV who recovered 8 and 9 days after infection, respectively. In C_{60}-Pip-treated mice (group 2) clinical manifestations of HSV-1 infection were observed throughout the entire observation period and the animals did not recover at the end of this period. A statistically significant decrease ($p < 0.05$) of the HSV-1-induced skin lesions was observed in groups 1 and 2 (Figure 9(a)). Mean score values in each group summarized within the observation period are given in Figure 8(b). A statistically significant decrease ($p < 0.05$) in herpetic skin lesions in comparison with the control (score 3.1 ± 0.3) was observed in group 1 (dnC_{60}, score 1.1 ± 0.3) and group 3 (ACV, score 0.8 ± 0.5).

3.2.4. Anti-HSV-1 antibody levels

The mean serum titer in control mouse group (4) on the 10th day after infection for survived mice was 1:1600

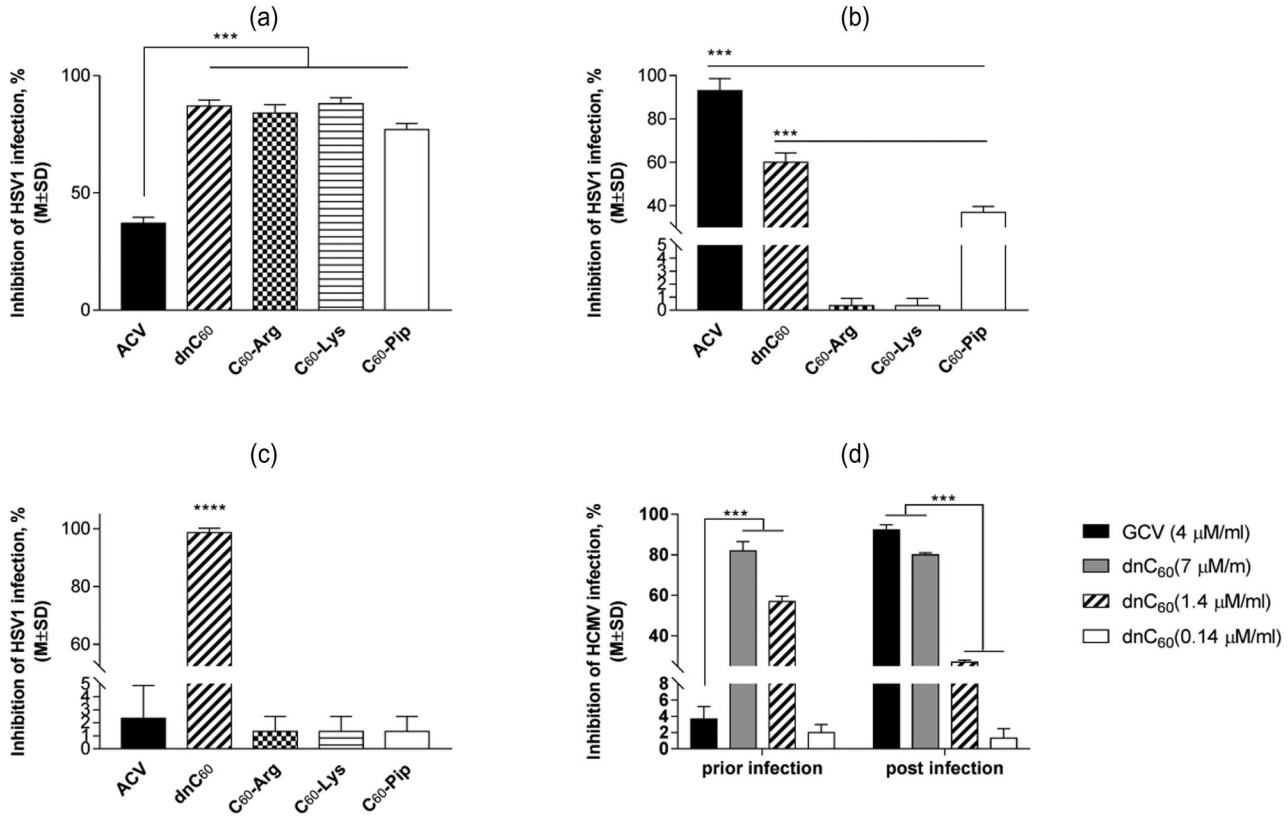

Figure 6. Antiviral activity of dnC_{60} and its amino acid derivatives in the cells infected with human herpesviruses. (a–c) Inhibition of HSV-1-infection (%). Vero cells were infected with HSV-1 at 0.01 PFU/cells and treated with test compounds at concentration 1.4 μM/ml as following: (a) 1 hour prior infection; (b) 1 hour post infection; (c) virus and compounds pre-incubated 1 hour and added to the cells (virucidal assay); each column represents the mean (M ± SD) of three experimental values; $^{***}p < 0.001$, $^{****}p < 0.0001$ (*t*-test); (d) effect of dnC_{60} against HCMV (%); HF cells were infected with HCMV at 0.001 PFU/cell and treated with different concentrations of dnC_{60} as following: 1 hour prior infection (left column block), 1 hour post infection (right column block); each column represents the mean (M ± SD) of three experimental values; $^{***}p < 0.001$ (*t*-test).

(Figure 9(c)). The dead infected animals from the same group had very low titer, 1:100, which practically did not differ from antibody level of non-infected animals. Serum assay of animals treating with dnC_{60}, C_{60}-Pip and ACV displayed titer levels 1:800, 1:200 and 1:400, respectively.

4. Discussion

In this study, we have demonstrated that an aqueous dispersion dnC_{60} possess the antiviral activity *in vitro* and *in vivo* against HSV-1 and in *vitro* against HCMV infections. The structural basis of most modern anti-herpetic drugs are acyclic nucleosides and their action is mainly aimed at suppressing the activity of virus DNA polymerase.[36] The structures of dnC_{60} are radically different from them, and the mechanism of its antiviral activity can be also dramatically different. There is information regarding the anti-herpetic activity of water-soluble C_{60}-phenylcarboxylate adducts in form of alkaline salts but their activity was descripted only for cell cultures and reported activities were not very significant.[10] Although water-soluble C_{60} adducts have been shown to exhibit good antiviral activity against some other infections (HIV, influenza, Ebola),[11,19,27,37] however the ndC_{60} containing unmodified fullerene differs markedly from the structure of these compounds, since their properties in strongly depend on the attached functional groups, how the benzene differs from its diverse derivatives. The dnC_{60} is a colloidal solution, cluster system, where each 50–100 nm cluster can contain many thousands of C_{60} molecules and whose size is close to a virus size (150–200 nm for HSV-1). These clusters contain not only fullerene, but also NMP in a close molar ratio. Note, that this organic solvent possesses a low toxicity upon oral, intradermal and inhalational administration and was approved by European commission and FDA as a constituent for production of preparations for medical purpose.[38,39]

We were interested in comparing the effects of unmodified fullerene and its derivatives, to what extent the contribution of C_{60} cage is decisive. Little is currently known about the mechanisms by which such a macromolecular system interferes with virus-cell interactions. To identify targets for the dnC_{60} action at different stages of virus life-cycle, selected compounds, dnC_{60} and C_{60}-Pip, were added to cell cultures: prior and post infection to model a prophylactic and therapeutic effects, respectively. All these compounds were able to significantly inhibit plaque formation of HSV-1 and HCMV when added prior to infection, while, they also had an effect when added after infection (Figure 6 and Table 1). Phenomenologically, these results suggest that both of these compounds can interact with different targets: with molecules on the cell surface, thereby preventing the virus from interacting with the cellular receptor, and hence blocking its entry into the cell. At the same time, dnC_{60} is able to suppress the infection after the virus enters the cell. Our

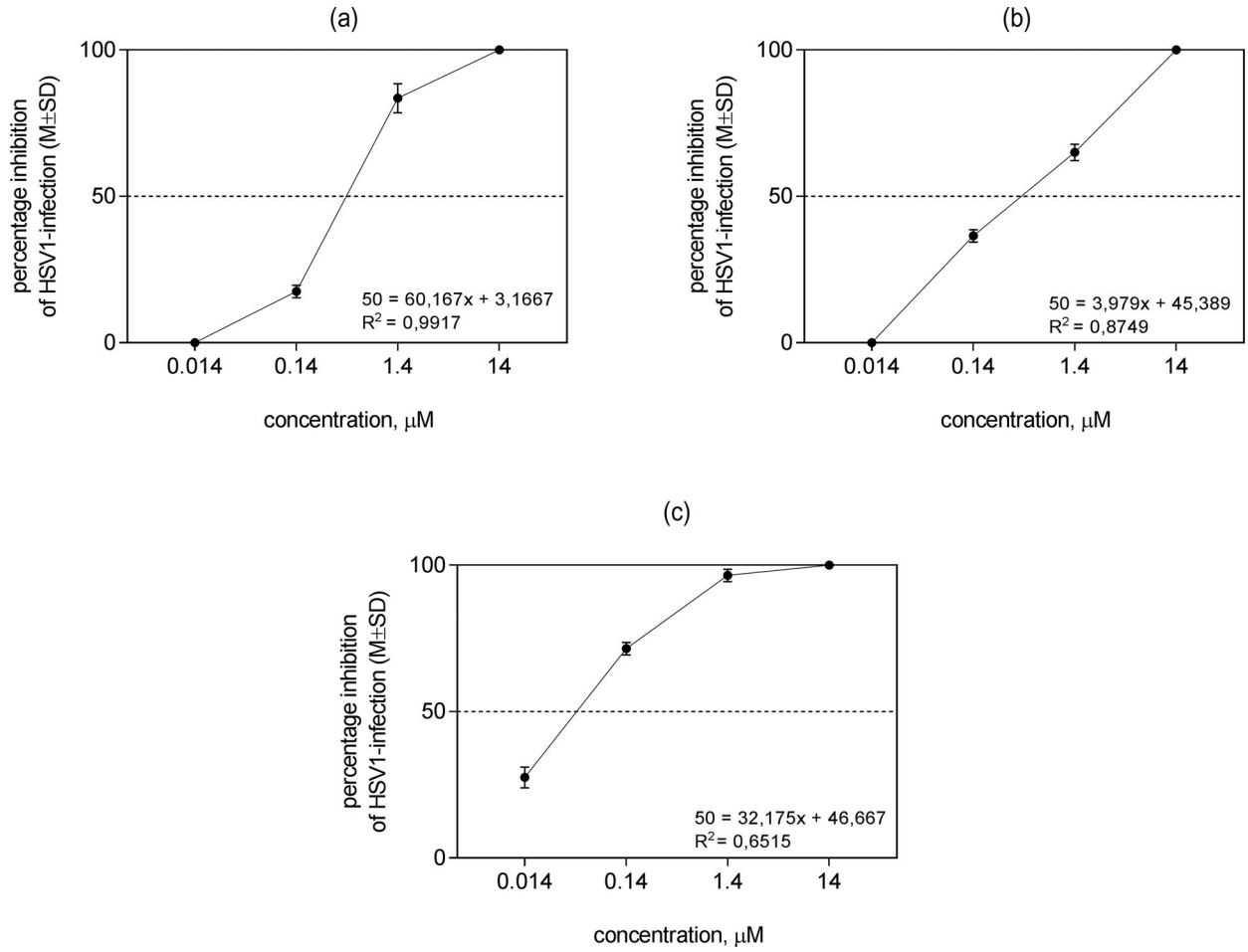

Figure 7. Determination of 50% inhibitory concentration (IC_{50}) of dnC_{60} against HSV-1. Vero cells were infected with HSV-1 at 0.01 PFU/cells and treated with various concentration of dnC_{60} as follows: (a) 1 hour prior infection; (b) 1 hour post infection; (c) virus and compounds were pre-incubated 1 hour and was added to the cells (virucidal assay); the percentage inhibition of HSV1-infection was calculated as follows: PI = [1 − (number of test plaques/number of control plaques)] × 100. The IC_{50} for dnC_{60} was calculated by regression analysis using Microsoft Excel software.

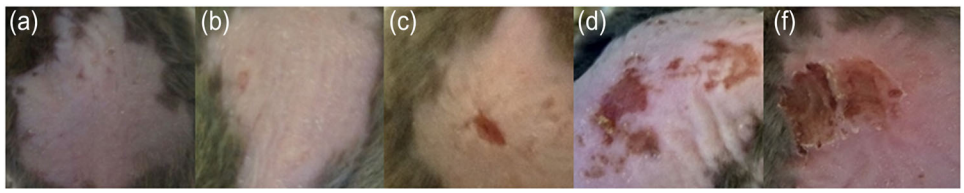

a – 0 (no visible change in the abrasion or surrounding tissue)
b – 1 (the earliest lesion)
c – 2 (erosion and/or ulceration in local region)
d – 3 (erosion and/or ulceration in several regions)
f – 4 (large open ulcerated lesion)
5 – (paralysis of hind limbs, loss of more than 20% of weight)
6 – death

Figure 8. Evaluation of clinical manifestations of cutaneous HSV-1 infection in infected mice. a–f correspond to scores 0–4, respectively.

data also indicate that dnC_{60} had a strong virucidal effect on the HSV-1 (SI = 1771) assuming that it may directly contribute to the inactivation of viral particles possibly by interfering with envelope or masking viral glycoproteins which are necessary for entering host cells. It is possibly that the whole nanoparticle exhibiting high adsorption properties and also individual dissociated C_{60} molecules can act as the active form.

Skin and mucous epithelium are primary sites for HSV-1 and HSV-2 entry and reactivation of viral infection. Cutaneous HSV-1 infection in humans and mice is characterized by replication of inoculated virus in skin and

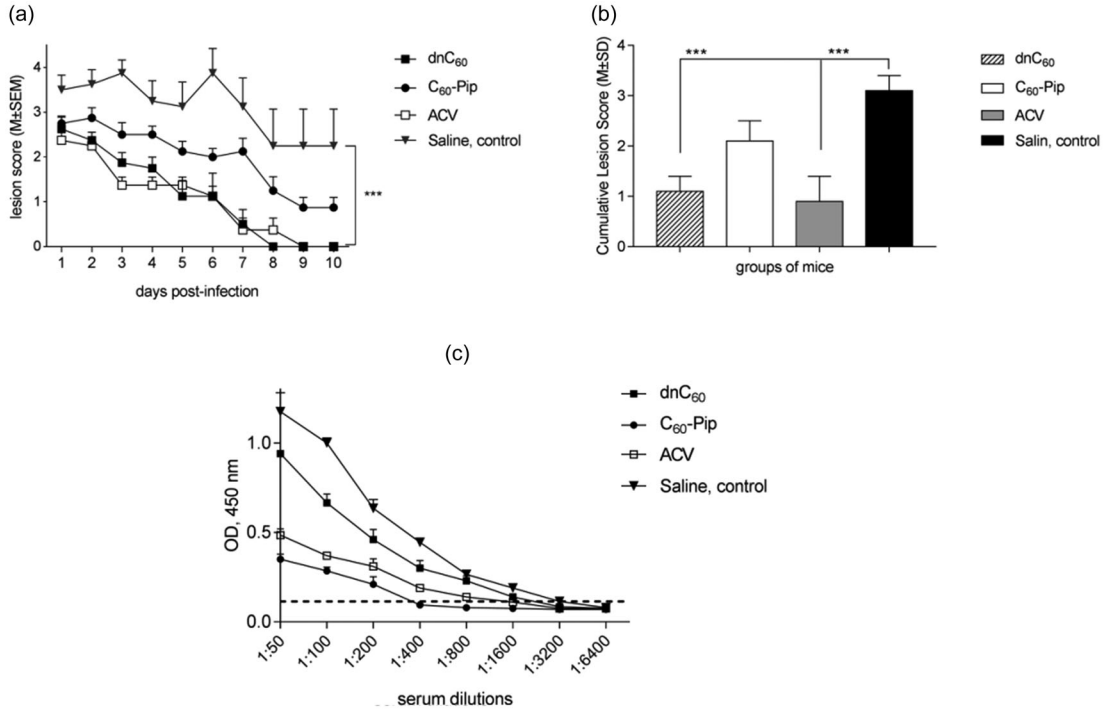

Figure 9. Comparative analysis of therapeutic (lesion) scores and anti-HSV antibody titers after treatment of HSV-infected mice with dnC_{60}, C_{60}-Pip, ACV and saline (negative control). (a) mice infected with HSV-1 were topically treated with dnC_{60}, C_{60}-Pip and ACV at doses 0.01 (closed squares), 0.05 (circles) and 5 (open squares) mg per mouse, respectively. Control mice were treated with saline (triangle). All the tested compounds were applied once daily from 0 to 3 days post-infection. The data are shown as the means ± SE using five animals per group; $^{***}p < 0.001$, compared to the control group (repeated measurements, ANOVA test); (b) the mean of cumulative lesion scores, data are expressed as the mean ± SD using five animals per group. $^{***}p < 0.001$, compared to the control group (*t*-test); (c) anti-HSV-1 antibodies (Ab) levels in mice sera; the dashed line shows anti-HSV-1 Ab level for naive mice.

mucous epithelium with subsequent migration into sensor ganglia where the virus can remain dormant for the entire life of the host. When reactivated, the virus is transported to primary infection sites, which causes skin rash and erosions spreading into adjacent tissues.[40,41] At the early stage (2–4 days after virus entry), cutaneous HSV-1 infection is limited to scarification site, then (day 5 and later) it spreads over the entire dermatome (skin area supplied by a single sensory nerve root).[42] In this study, maximum lesions formation was observed in control mice on days 3 and 6 post infection, which may reflect two phases of HSV-1 replication in the skin (Figure 8(a)). In dnC_{60}-treated mice, as in ACV-treated mice, the clinical manifestations of skin HSV-1-infection were minimal, and a statistical decrease of lesion formation was observed 2 days after infection, full recovery was achieved on days 8 and 9 after infection (Figure 8(a,b), respectively). It should be noted that dnC_{60} showed therapeutic anti-HSV-1 activity 24 hours earlier and at a concentration 500-fold lower than that of ACV.

To evaluate the level of virus repression in cell under the dnC_{60} action, the model of CMV infection *in vitro* was used. The expression levels of HCMV mRNAs of three important proteins were assessed: (a) UL122, immediate-early HCMV protein IE2 (86-kDa), one of critical regulators of virus replication; (b) UL83, structural protein pp65, a major protein from viral tegument (layer localized between the shell and capsid) and (c) UL54, viral DNA polymerase. The assay showed that the expression of all the studied HCMV genes in the presence of dnC_{60} was significantly reduced, more than an order of magnitude ($p < 0.05$) (Table 2). The greatest change (by a factor of 22) was observed in the activity of IE2 gene, which triggers a cascade of events leading to the death of infected cells. Thus, it was shown that the antiviral effect of fullerene at the molecular level was manifested in the suppression of transcriptional regulatory (UL122) and structural viral genes involved in the mechanisms of replication of the HCMV genome (UL54) and post-replicative processes of viral particles formation (UL83). However, molecular events leading to such consequences are not yet known and need to be clarified.

Currently there is a lot of data regarding an antioxidant activity of aqueous dispersions of fullerene C_{60} and C_{60} derivatives,[7,8,12] a property that unites them and may underlie the mechanism of action. It can be assumed that fullerene as a strong electron acceptor can affect the state of the redox potential in host cells because the viral infection is accompanied by an increase in the level of ROS in the cells which contributes to the replication of the virus.[43–47] On the other hand, it was shown that the main mechanism of the *in vitro* action of polyphenolic antioxidant echinochrome A is the direct inactivation of viral particles inhibiting their interaction with host cells, as well as irreversible damage of the viral envelope proteins. Since fullerene, like echinochrome A, is capable of strong π-π stacking interactions which may be responsible for the virion inactivation, it can be assumed that their mechanisms are similar (virucidal effect).[48] Also previously it was showed that when BALB/c mice were injected either subcutaneous or epicutaneous with

Table 2. Analysis of the transcription of three CMV genes.

	Relative levels of mRNA expression		
Gene	Positive control, CMV infected cells	Under the action of dnC_{60} on CMV infected cells	Multiplicity of effect
UL122	34.64 ± 10.36	1.5 ± 0.42	22.6
UL83	300 ± 71	25 ± 8.3	12.0
UL54	1.43 ± 0.35	0.13 ± 0.01	11.0

dnC_{60}, the IFN-γ levels (mRNA) were greatly increased by matching with the treatment by PBS only.[22] The IFN-γ is known to significantly inhibit HSV-1 infection in epidermal cells playing an important immunologic role in recurrent herpes simplex lesions.[49]

To evaluate the role of the antibody (Ab) immune response in protecting against a skin HSV-1 infection, the correlation between titers of HSV-1 specific IgG and levels of viral infection was studied. The Ab production was observed in the majority of mice infected with HSV-1 remained alive, and vice versa, no antibodies against HSV-1 were detected in dead mice. It is interesting, no animals with high anti-HSV-1 titer died, but none of them recovered completely. For instance, occasional skin erosions were observed in survived control mice (titer 1:1600) on day 10, while all dnC_{60}- and ACV-treated mice (titers 1:800 and 1:400, respectively) survived and had no herpetic skin lesions by that time. Thus, these data suggest that there is some protective activity of anti-HSV Abs but their role is controversial, and other immune mechanisms should be triggered for recovery from the infection.

In conclusion, we can emphasize that the activity of aqueous dispersion of unmodified fullerene, dnC_{60} in all tests exceeds the activity of C_{60} derivatives including also markedly lower cytotoxicity. Regarding the prospects for the therapeutic use of C_{60} adducts, one of the significant drawbacks is the uncertainty of their chemical structure due to polyaddition reactions to the C_{60} core with the formation of a plume of products, obtaining a homogeneous product is very difficult. In total, the observed effects of dnC_{60} are as follows: (a) prevention of HSV-1 and HCMV infections *in vitro*; (b) suppression of HSV-1 activity via the virucidal effect; (c) *in vivo* antiviral activity in most tests exceeded the activity of both C_{60} derivatives and ACV. Concentrated C_{60} solutions can be obtained on a large scale up using well-developed ultrafiltration technology. These properties render the dnC60 as a promising candidate for the creation of novel antiviral drug capable effectively of inhibiting herpesviral infections. At the same time, future research is needed to clarify the mechanisms of the antiviral effect of fullerene-based substances.

Authors' contributions

RK, EM, ND, NF, YC and KY carried out work with animals, analyzed the course of a viral infection, provided immunoassay and statistical processing. SA, ET, NS and EB have prepared the ndC_{60} and C_{60} derivatives with their characterization. RS performed the real-time PCR analysis; SA, AK, MK and AG have made substantial contributions to conception, design, and interpretation of data and given final approval of the version to be published. All authors read and approved the final manuscript.

Acknowledgements

The authors thank technical specialist I. Solovyov (Teskan Ltd., St. Petersburg, Russia) for providing electronic images, Artem Shatilov (NRC Institute of Immunology) for providing some analytical data on the dnC_{60}.

Disclosure statement

The authors declare that they have no competing interests.

Funding

This study did not receive any specific grant from funding agencies in the public or nonprofit sector. Partial support was received from company C_{60}Bio Ltd. (some reagents and instruments).

ORCID

Ruslan Simonov http://orcid.org/0000-0002-7706-8228

References

[1] Herpes simplex virus. https://www.who.int/news-room/fact-sheets/detail/herpes-simplex-virus (accessed 31 January 2017).

[2] Looker, K. J.; Magaret, A. S.; May, M. T.; Turner, K. M. E.; Vickerman, P.; Gottlieb, S. L.; Newman, L. M. Global and Regional Estimates of Prevalent and Incident Herpes Simplex Virus Type 1 Infections in 2012. *PLoS One* **2015**, *10*, e0140765. DOI: 10.1371/journal.pone.0140765.

[3] Jiang, Y. C.; Feng, H.; Lin, Y. C.; Guo, X. R. New Strategies against Drug Resistance to Herpes Simplex Virus. *Int. J. Oral Sci.* **2016**, *8*, 1–6. DOI: 10.1038/ijos.2016.3.

[4] Piret, J.; Boivin, G. Resistance of Herpes Simplex Viruses to Nucleoside Analogues: mechanisms, Prevalence, and Management. *Antimicrob. Agents Chemother.* **2011**, *55*, 459–472. DOI: 10.1128/AAC.00615-10.

[5] Piret, J.; Boivin, G. Antiviral Drug Resistance in Herpesviruses Other than Cytomegalovirus. *Rev. Med. Virol.* **2014**, *3*, 186–218. DOI: 10.1002/rmv.1787.

[6] Andreev, I.; Petrukhina, A.; Garmanova, A.; Babakhin, A.; Andreev, S.; Romanova, V.; Troshin, P.; Troshina, O.; DuBuske, L. Penetration of Fullerene C_{60} Derivatives through Biological Membranes. *Fullerenes Nanotubes Carbon Nanostruct.* **2008**, *16*, 89–102. DOI: 10.1080/15363830701885831.

[7] Lao, F.; Li, W.; Han, D.; Qu, Y.; Liu, Y.; Zhao, Y.; Chen, C. Fullerene Derivatives Protect Endothelial Cells against NO-Induced Damage. *Nanotechnology* **2009**, *20*, 225103. DOI: 10.1088/0957-4484/20/22/225103.

[8] Kadowaki, A.; Iwamoto, S.; Yamauchi, R. The Antioxidative Effect of Fullerenes during the Peroxidation of Methyl Linoleate in Toluene. *Biosci. Biotechnol. Biochem.* **2012**, *76*, 212–214. DOI: 10.1271/bbb.110739.

[9] Chen, T.; Li, Y. Y.; Zhang, J. L.; Xu, B.; Lin, Y.; Wang, C. X.; Guan, W. C.; Wang, Y. J.; Xu, S. Q. Protective Effect of C(60)-Methionine Derivate on Lead-Exposed Human SH-SY5Y Neuroblastoma Cells. *J. Appl. Toxicol.* **2011**, *31*, 255–261. DOI: 10.1002/jat.1588.

[10] Fedorova, N. E.; Klimova, R. R.; Tulenev, Y. A.; Chichev, E. V.; Kornev, A. B.; Troshin, P. A.; Kushch, A. A. Carboxylic Fullerene C60 Derivatives: Efficient Microbicides against Herpes Simplex Virus and Cytomegalovirus Infections in Vitro. *Mendeleev Commun.* **2012**, *22*, 254–256. DOI: 10.1016/j.mencom.2012.09.009.

[11] Shoji, M.; Takahashi, E.; Hatakeyama, D.; Iwai, Y.; Morita, Y.; Shirayama, R.; Echigo, N.; Kido, H.; Nakamura, S.; Mashino, T.; et al. Anti-Influenza Activity of c60 Fullerene Derivatives. *PLoS One* **2013**, *8*, e66337. DOI: 10.1371/journal.pone.0066337.

[12] Barron, A. R. [60]Fullerene-Peptides: bionanoconjugates with Structural and Chemical Diversity. *J. Enzyme Inhib. Med. Chem.* **2016**, *31*, 164–176. DOI: 10.1080/14756366.2016.1177524.

[13] Kataoka, H.; Ohe, T.; Takahashi, K.; Nakamura, S.; Mashino, T. Novel Fullerene Derivatives as Dual Inhibitors of Hepatitis C Virus NS5B Polymerase and NS3/4A Protease. *Bioorg. Med. Chem. Lett.* **2016**, *26*, 4565–4567. DOI: 10.1016/j.bmcl.2016.08.086.

[14] Labille, J.; Masion, A.; Ziarelli, F.; Rose, J.; Brant, J.; Villiéras, F.; Pelletier, M.; Borschneck, D.; Wiesner, M. R.; Bottero, J.-Y. Hydration and Dispersion of C_{60} in Aqueous Systems: The Nature of Water-Fullerene Interactions. *Langmuir* **2009**, *25*, 11232–11235. DOI: 10.1021/la9022807.

[15] Andreev, S.; Purgina, D.; Bashkatova, B.; Garshev, A.; Maerle, A.; Andreev, I.; Osipova, N.; Shershakova, N.; Khaitov, M. Study of Fullerene Aqueous Dispersion Prepared by Novel Dialysis Method. Simple Way to Fullerene Aqueous Solution. *Fullerenes Nanotubes Carbon Nanostruct.* **2015**, *23*, 792–800. DOI: 10.1080/1536383X.2014.998758.

[16] Gharbi, N.; Pressac, M.; Hadchouel, M.; Szwarc, H.; Wilson, S. R.; Moussa, F. [60]Fullerene is a Powerful Antioxidant in Vivo with No Acute or Subacute Toxicity. *Nano Lett.* **2005**, *5*, 2578–2585. DOI: 10.1021/nl051866b.

[17] Witte, P.; Beuerle, F.; Hartnagel, U.; Lebovitz, R.; Savouchkina, A.; Sali, S.; Guldi, D.; Chronakis, N.; Hirsch, A. Water Solubility, Antioxidant Activity and Cytochrome C Binding of Four Families of Exohedral Adducts of C60 and C70. *Org. Biomol. Chem.* **2007**, *5*, 3599–3613. DOI: 10.1039/b711912g.

[18] Prylutskyy, Y. I.; Petrenko, V. I.; Ivankov, V. I.; Kyzyma, O. A.; Bulavin, L. A.; Litsis, O. O.; Evstigneev, M. P.; Cherepanov, V. V.; Naumovets, A. G.; Ritter, U. On the Origin of C_{60} Fullerene Solubility in Aqueous Solution. *Langmuir* **2014**, *30*, 3967–3970. DOI: 10.1021/la404976k.

[19] Goodarzi, S.; Da Ros, T.; Conde, J.; Sefat, F.; Mozafari, M. Fullerene: Biomedical Engineers Get to Revisit an Old Friend. *Mater. Today* **2017**, *20*, 460–480. DOI: 10.1016/j.mattod.2017.03.017.

[20] Piotrovsky, L. B.; Kiselev, O. I. *Fullerenes in Biology*. SPb.: Rostock, **2006**. 336 p.

[21] Nosik, N. N.; Kondrashina, N. G.; Grigor'eva, AIu.; Lialina, I. K.; Rasnetsov, L. D. Fullevir: In Vitro and in Vivo Antiherpetic Activity. *Vopr. Virusol.* **2009**, *54*, 15–18. (in Russian).

[22] Shershakova, N.; Baraboshkina, E.; Andreev, S.; Purgina, D.; Struchkova, I.; Kamyshnikov, O.; Nikonova, A.; Khaitov, M. Anti-Inflammatory Effect of Fullerene C_{60} in a Mice Model of Atopic Dermatitis. *J. Nanobiotechnol.* **2016**, *14*, 8. DOI: 10.1186/s12951-016-0159-z.

[23] Mchedlov-Petrossyan, N. O. Fullerenes in Liquid Media: An Unsettling Intrusion into the Solution Chemistry. *Chem. Rev.* **2013**, *113*, 5149–5193. DOI: 10.1021/cr3005026.

[24] Andrievsky, G. V.; Kosevich, M. V.; Vovk, O. M.; Shelkovsky, V. S.; Vashchenko, L. A. On the Production of an Aqueous Colloidal Solution of Fullerenes. *J. Chem. Soc. Chem. Commun.* **1995**, *12*, 1281–1282. DOI: 10.1039/c39950001281.

[25] Shershakova, N.; Kuks, E.; Turetskiy, E.; Kamishnikov, O.; Andreev, S.; Khaitov, M. Fullerene C60 Reduces the Allergic Inflammation in Food Allergy Mouse Model. *Allergy* **2018**, *73*, 787.

[26] Bakry, R.; Vallant, R. M.; Najam-Ul-Haq, M.; Rainer, M.; Szabo, Z.; Huck, C. W.; Bonn, G. K. Medicinal Applications of Fullerenes. *Int. J. Nanomed.* **2007**, *2*, 639–649.

[27] Castro, E.; Hernandez, G; Zavala, G; Echegoyen, L. Fullerenes in Biology and Medicine. *J. Mater. Chem. B* **2017**, *5*, 6523–6535. DOI: 10.1039/c7tb00855d.

[28] Klimova, R. R.; Momotyuk, E. D.; Demidova, N. A.; Chernoryzh, YaYu.; Koval, V. S.; Ivanov, A. A.; Zhoze, A. L.; Kushch, A. A. Dimeric Bisbenzimidazoles Suppress Infections Caused by the Herpes Simplex Virus and Human Cytomegalovirus in Cell Cultures. *Vopr. Virusol.* **2017**, *62*, 162–168. (in Russian). DOI: 10.18821/0507-4088-2017-62-4-162-168.

[29] Docherty, J. J.; Smith, J. S.; Fu, M. M.; Stoner, T.; Booth, T. Effect of Topically Applied Resveratrol on Cutaneous Herpes Simplex Virus Infections in Hairless Mice. *Antivir. Res.* **2004**, *61*, 19–26. DOI: 10.1016/j.antiviral.2003.07.001.

[30] Lipipun, V.; Sasivimolphan, P.; Yoshida, Y.; Daikoku, T.; Sritularak, B.; Ritthidej, G.; Likhitwitayawuid, K.; Pramyothin, P.; Hattori, M.; Shiraki, K. Topical Cream-Based Oxyresveratrol in the Treatment of Cutaneous HSV-1 Infection in Mice. *Antiviral Res.* **2011**, *91*, 154–160. DOI: 10.1016/j.antiviral.2011.05.013.

[31] Klimova, R. R.; Kozlov, AIu.; Shingarova, L. N.; Nekrasova, O. V.; Boldyreva, E. F.; Guseva, T. S.; Parshina, O. V.; Malinovskaia, V. V.; Novikov, V. V.; Kushch, A. A. The Effect of the Tumor Necrosis Factor DNA on the Immune Response in DNA Immunization against the Herpes Simplex Virus. *Mol. Biol. (Mosk.)* **2004**, *38*, 333–342. (in Russian).

[32] Tomchuk, A. A.; Shershakova, N. N.; Andreev, S. M.; Turetskiy, E. A.; Ivankov, O. I.; Kyzyma, O. A.; Tomchuk, O. V.; Avdeev, M. V. C_{60} and C_{60}-Arginine Aqueous Solutions: In Vitro Toxicity and Structural Study. *Fullerenes Nanotubes Carbon Nanostruct.* DOI: 10.1080/1536383X.2019.1697242.

[33] Rogozhin, S. V.; Davidovich, YuA.; Andreev, S. M.; Mironova, N. V.; Yurtanov, A. I. Preparation of Trimethylsilyl Derivatives of Amino Acids and Peptides for Peptide Synthesis. *Russ. Chem. Bull.* **1974**, *23*, 1789–1792. DOI: 10.1007/BF00923213.

[34] Isobe, H.; Nakanishi, W.; Tomita, N.; Jinno, S.; Okayama, H.; Nakamura, E. Gene Delivery by Aminofullerenes: Structural Requirements for Efficient Transfection. *Chem. Asian J.* **2006**, *1*, 167–175. DOI: 10.1002/asia.200600051.

[35] Piotrovsky, L. B.; Milman, B. L.; Nikolaev, D. N.; Lugovkina, N. V.; Litasova, E. V.; Dumpis, M. A. Characterization of Fullerene Derivatives by MALDI LIFT-TOF/TOF Mass Spectrometry. *Nanosyt. Phys. Chem. Math.* **2014**, *5*, 76–80.

[36] Zinser, E.; Krawczyk, A.; Mühl-Zürbes, P.; Aufderhorst, U.; Draßner, C.; Stich, L.; Zaja, M.; Strobl, S.; Steinkasserer, A.; Heilingloh, C. S. A New Promising Candidate to Overcome Drug Resistant Herpes Simplex Virus Infections. *Antiviral Res.* **2018**, *149*, 202–210. DOI: 10.1016/j.antiviral.2017.11.012.

[37] Saleh, N. A. The QSAR and Docking Calculations of Fullerene Derivatives as HIV-1 Protease Inhibitors. Spectrochim. *Acta Part A Mol. Biomol. Spectrosc.* **2014**, *136*, 1523–1529. DOI: 10.1016/j.saa.2014.10.045.

[38] Sanghvi, R.; Narazaki, R.; Machatha, S. G.; Yalkowsky, S. H. Solubility Improvement of Drugs Using N-Methyl Pyrrolidone. *AAPS PharmSciTech.* **2008**, *9*, 366–376. DOI: 10.1208/s12249-008-9050-z.

[39] Bartsch, W.; Sponer, G.; Dietmann, K.; Fuchs, G. Acute Toxicity of Various Solvents in the Mouse and Rat. *Arzneimittelforschung* **1976**, *26*, 1581–1583.

[40] van Lint, A.; Ayers, M.; Brooks, A. G.; Coles, R. M.; Heath, W. R.; Carbone, F. R. Herpes Simplex Virus-Specific CD8+ T

Cells Can Clear Established Lytic Infections from Skin and Nerves and Can Partially Limit the Early Spread of Virus after Cutaneous Inoculation. *J. Immunol.* **2004**, *172*, 392–397. DOI: 10.4049/jimmunol.172.1.392.

[41] Roizman, B.; Whitley, R. J. An Inquiry into the Molecular Basis of HSV Latency and Reactivation. *Annu. Rev. Microbiol.* **2013**, *67*, 355–374. DOI: 10.1146/annurev-micro-092412-155654.

[42] Bedoui, S.; Whitney, P. G.; Waithman, J.; Eidsmo, L.; Wakim, L.; Caminschi, I.; Allan, R. S.; Wojtasiak, M.; Shortman, K.; Carbone, F. R.; et al. Cross-Presentation of Viral and Self Antigens by Skin-Derived CD103+ Dendritic Cells. *Nat. Immunol.* **2009**, *10*, 488–495. DOI: 10.1038/ni.1724.

[43] Valyi-Nagy, T.; Dermody, T. S. Role of Oxidative Damage in the Pathogenesis of Viral Infections of the Nervous system. *Histol. Histopathol.* **2005**, *20*, 957–967.

[44] Gullberg, R. C.; Jordan Steel, J.; Moon, S. L.; Soltani, E.; Geiss, B. J. Oxidative Stress Influences Positive Strand RNA Virus Genome Synthesis and Capping. *Virology* **2015**, *475*, 219–229. DOI: 10.1016/j.virol.2014.10.037.

[45] Annunziata, G.; Maisto, M.; Schisano, C.; Ciampaglia, R.; Narciso, V.; Tenore, G. C.; Novellino, E. Resveratrol as a Novel anti-Herpes Simplex Virus Nutraceutical Agent: An Overview. *Viruses* **2018**, *10*, 473. DOI: 10.3390/v10090473.

[46] Chen, X.; Qiao, H.; Liu, T.; Yang, Z.; Xu, L.; Xu, Y.; Ge, H. M.; Tan, R. X.; Li, E. Inhibition of Herpes Simplex Virus Infection by Oligomeric Stilbenoids through ROS Generation. *Antivir. Res.* **2012**, *95*, 30–36. DOI: 10.1016/j.antiviral.2012.05.001.

[47] Sebastiano, M.; Chastel, O.; de Thoisy, B.; Eens, M.; Costantini, D. Oxidative Stress Favors Herpes Virus Infection in Vertebrates: A Meta-Analysis. *Curr. Zool.* **2016**, *62*, 325–332. DOI: 10.1093/cz/zow019.

[48] Fedoreyev, S. A.; Krylova, N. V.; Mishchenko, N. P.; Vasileva, E. A.; Pislyagin, E. A.; Iunikhina, O. V.; Lavrov, V. F.; Svitich, O. A.; Ebralidze, L. K.; Leonova, G. N. Antiviral and Antioxidant Properties of Echinochrome A. *Mar. Drugs* **2018**, *16*, 509. DOI: 10.3390/md16120509.

[49] Mikloska, Z.; Cunningham, A. L. J. Alpha and Gamma Interferons Inhibit Herpes Simplex Virus Type 1 Infection and Spread in Epidermal Cells after Axonal Transmission. *Journal of Virology* **2001**, *75*, 11821–11826. DOI: 10.1128/JVI.75.23.11821-11826.2001.